Supplementary Information

Strengthening Non-Pre-Irradiated Near-Infrared Mechanoluminescence of CaZnOS:Nd^{3+} by Mn^{2+} coactivation for Biomechanical Imaging

Jianxiong Lei, Wei Li, Yiqian Tang, Yiyu Cai, Shanshan Wang, Kunpeng Dou, Jun-Cheng Zhang**

College of Physics and Optoelectronic Engineering, Ocean University of China, Qingdao 266100, China

Email: wangshanshan@ouc.edu.cn (S. Wang); zhangjuncheng@ouc.edu.cn (J.-C. Zhang).

Table of Contents

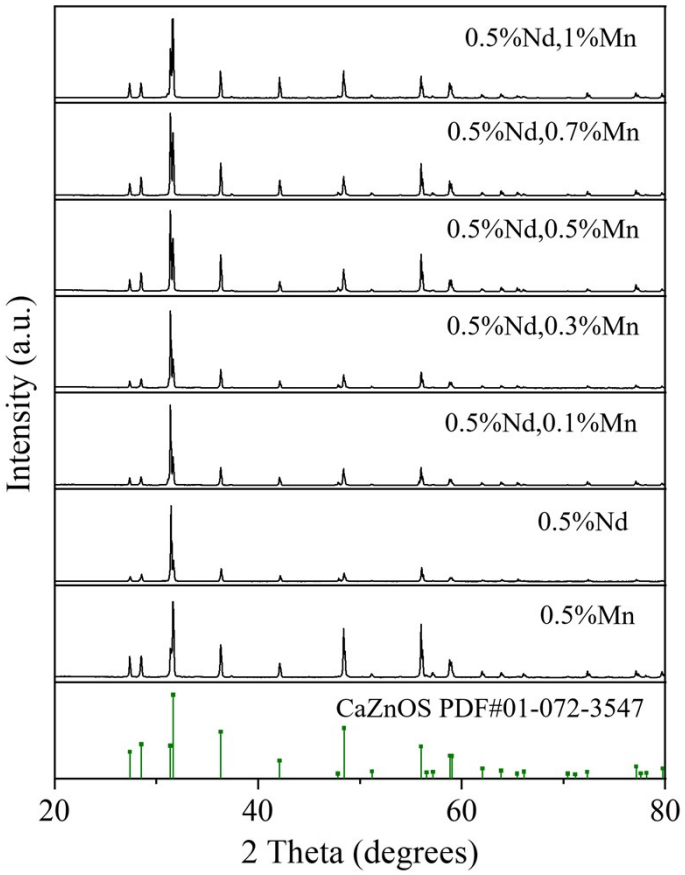

Fig. S1 Powder XRD patterns of CaZnOS:Nd^{3+},Mn^{2+} series with different Nd^{3+} and Mn^{2+} concentrations. None of impurity lines have been detected. It indicates that the synthesized phosphors are the single phase of CaZnOS.

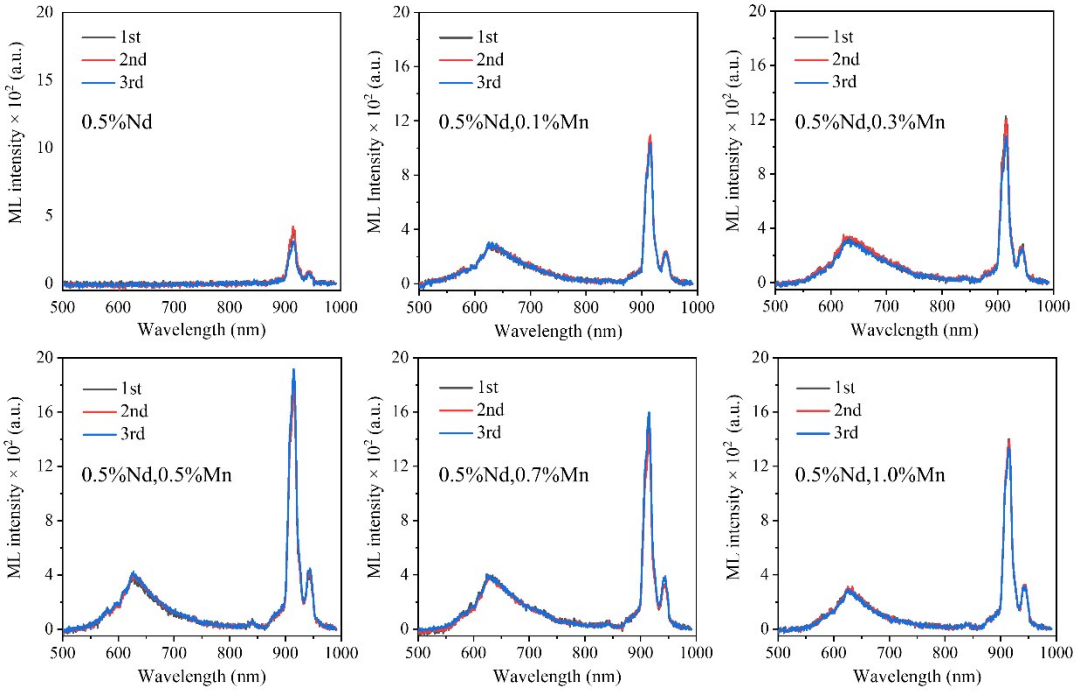

Fig. S2 ML spectra of CaZnOS:Nd^{3+},Mn^{2+} series collected in a compressive test (0–1000 N, 5 mm/min). For each component of the CaZnOS:Nd^{3+},Mn^{2+} series, three fresh samples were tested separately for error analysis. The results show high repeatability of the compression-induced ML spectra for the fresh samples.

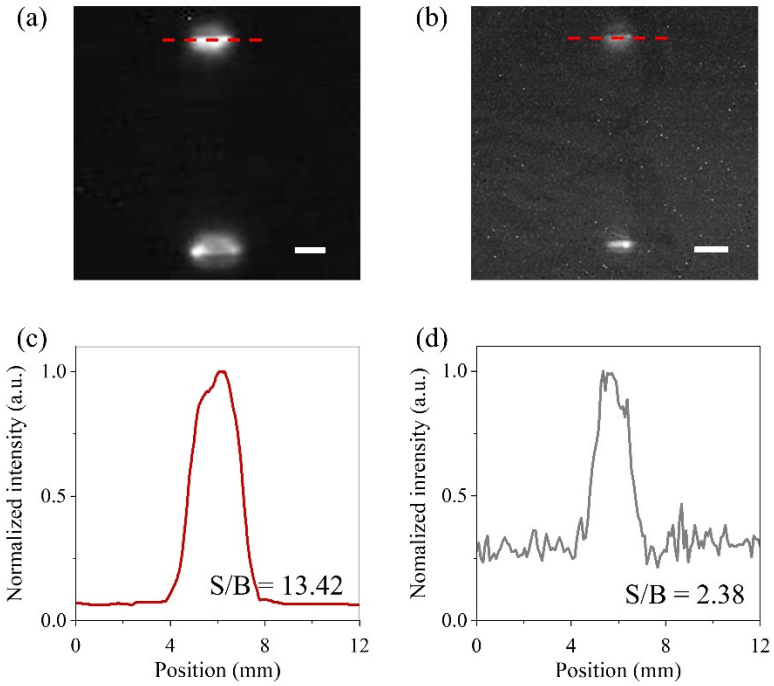

Fig. S3 Compression-induced NIR-ML images of CaZnOS:0.5%Nd^{3+},0.5%Mn^{2+} (a) and CaZnOS:0.5%Nd^{3+} (b) with the corresponding SBR analysis shown in (c) and (d). Scale bars: 3 mm.

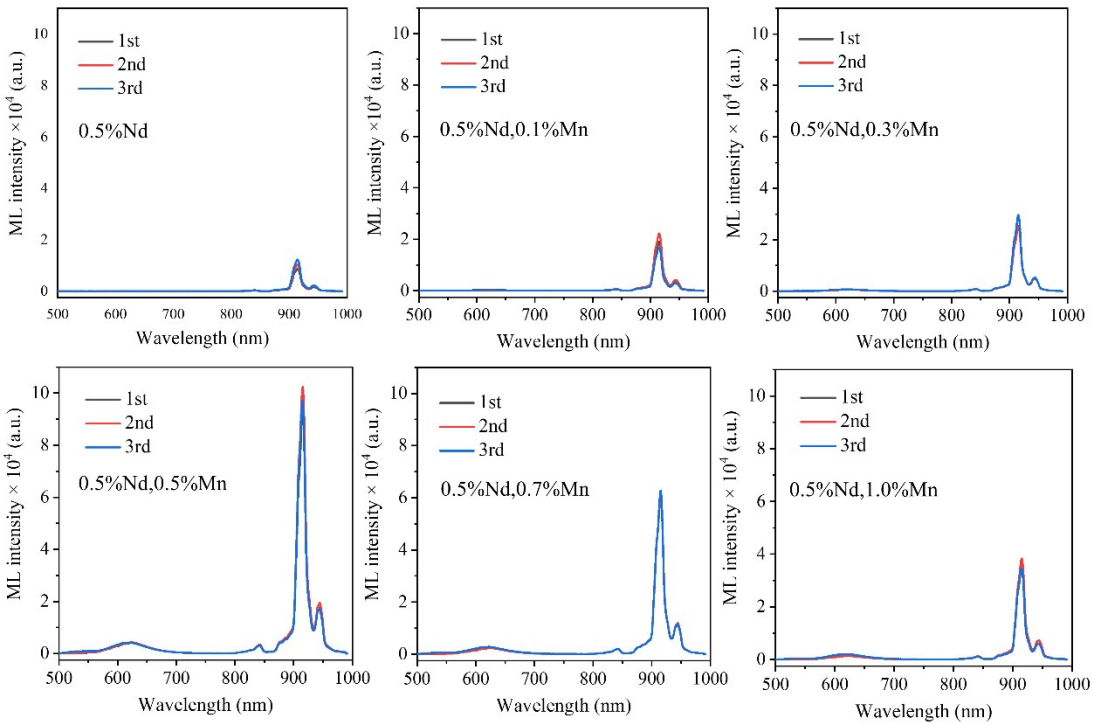

Fig. S4 ML spectra of CaZnOS:Nd^{3+},Mn^{2+} series collected in a frictional test (5 N, 100 r/min). For each component of the CaZnOS:Nd^{3+},Mn^{2+} series, three fresh samples were tested separately for error analysis. The results show high repeatability of the friction-induced ML spectra for the fresh samples.

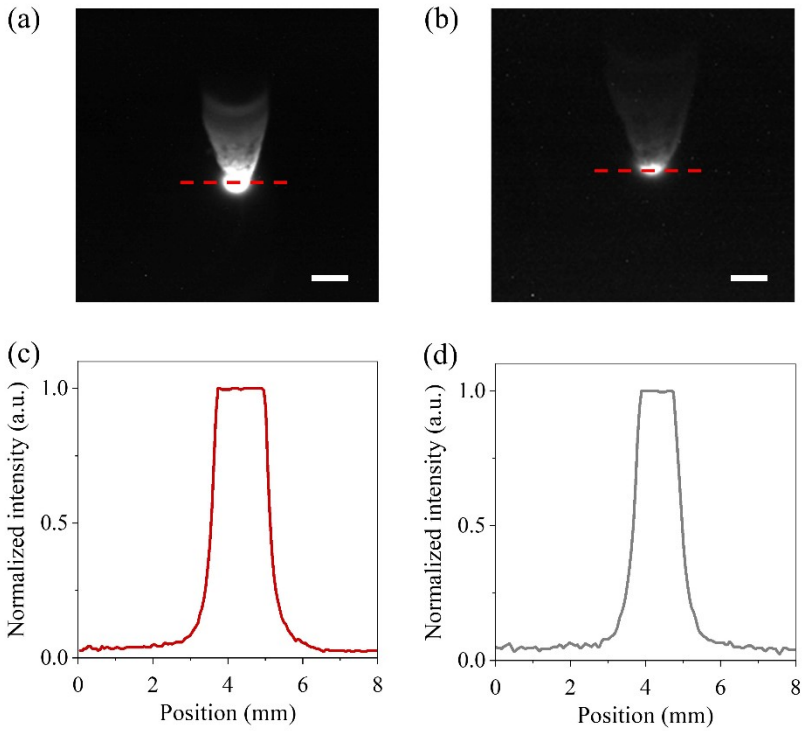

Fig. S5 Friction-induced NIR ML images of CaZnOS:0.5%Nd^{3+},0.5%Mn^{2+} (a) and CaZnOS:0.5%Nd^{3+} (b) with the corresponding SBR analysis shown in (c) and (d). Scale bars: 3 mm. It should be noted that the NIR ML intensity exceeds the threshold of the NIR camera used, resulting in the platform in (c) and (d), respectively. Although it is difficult to directly compare the NIR ML intensity due to the platform, it can be inferred that the NIR ML of CaZnOS:0.5%Nd^{3+},Mn^{2+} should have higher trend based on the wider platform in (c) relative to (d). On the other hand, it can be clearly observed that the background noise of the NIR ML images of CaZnOS:0.5%Nd^{3+},0.5%Mn^{2+} (c) is lower than that of CaZnOS:0.5%Nd^{3+} (d). Therefore, we can reasonably infer that the use of CaZnOS:0.5%Nd^{3+},0.5%Mn^{2+} in this experiment effectively improves the SBR of the NIR ML images.

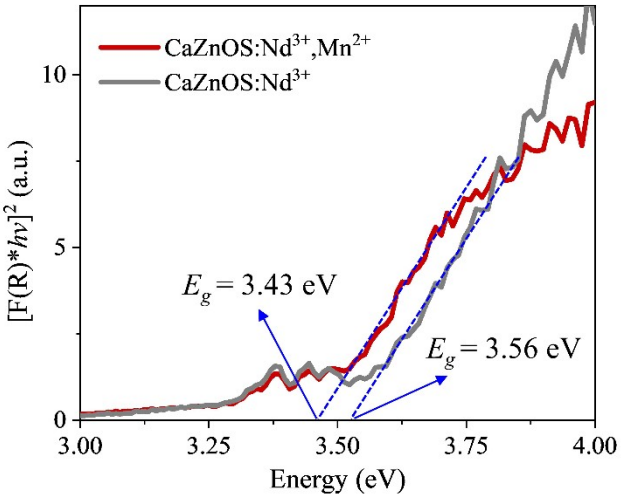

Fig. S6 Derivation of the optical bandgap of CaZnOS:0.5%Nd^{3+},0.5%Mn^{2+}. The results show that Mn^{2+} doping reduces the bandgap from 3.56 eV (CaZnOS:0.5%Nd^{3+}) to 3.43 eV (CaZnOS:0.5%Nd^{3+},0.5%Mn^{2+}).

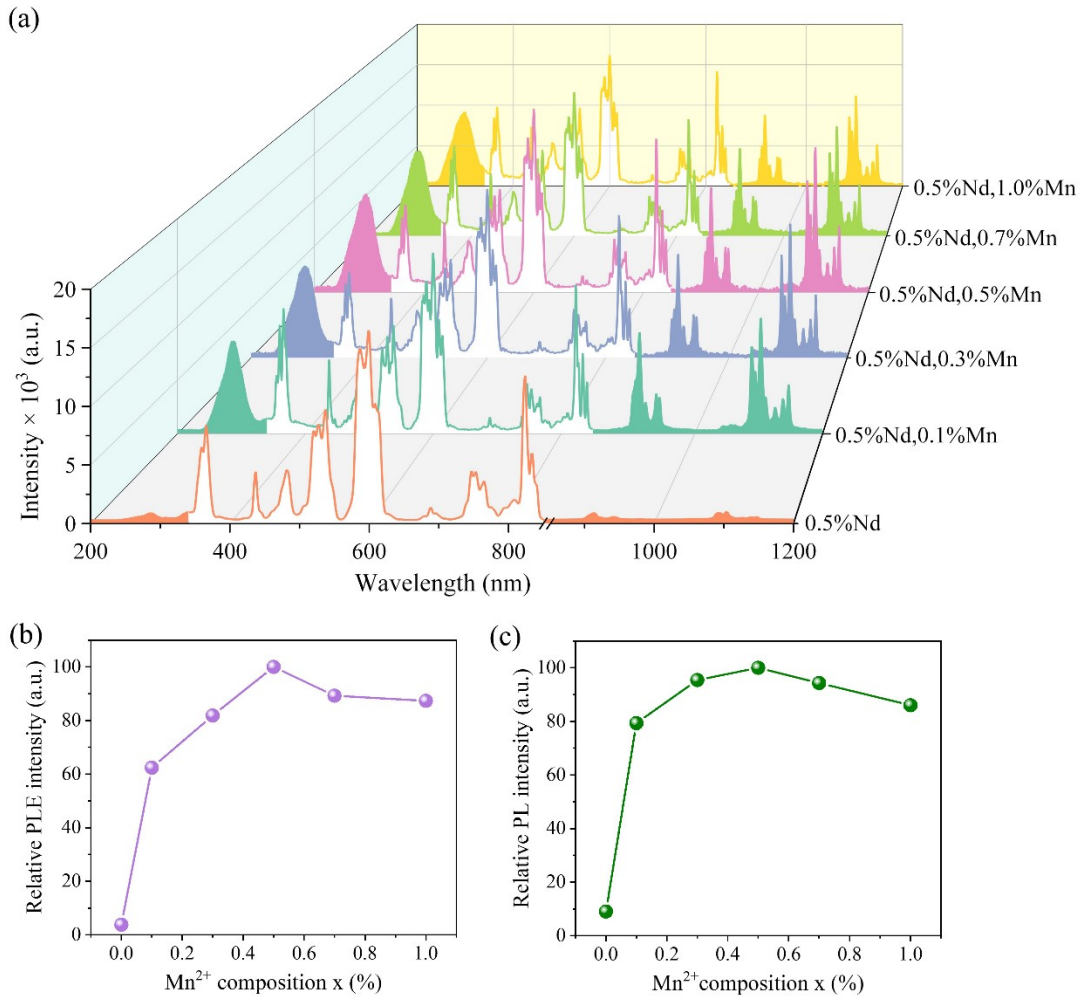

Fig. S7 (a) PL excitation (PLE) and emission spectra of CaZnOS:Nd^{3+},Mn^{2+} series (λ_{ex} = 277 nm, λ_{em} = 914 nm). (b) and (c) Relative PLE intensity of host and NIR PL intensity of Nd^{3+} as a function of Mn^{2+} concentration, respectively. The results indicate that the PLE band of the host (marked with colored shading) is significantly increased by Mn^{2+} doping, resulting in the enhanced NIR emission from Nd^{3+}. Furthermore, the optimal Mn^{2+} concentration for increasing the NIR PL of Nd^{3+} is 0.5 mol%, which is the same as the optimal concentration for increasing the NIR ML of Nd^{3+} (Figures 2b and 3b). It suggests that the enhancement of PL and ML should go through the same pathway of energy transfer.

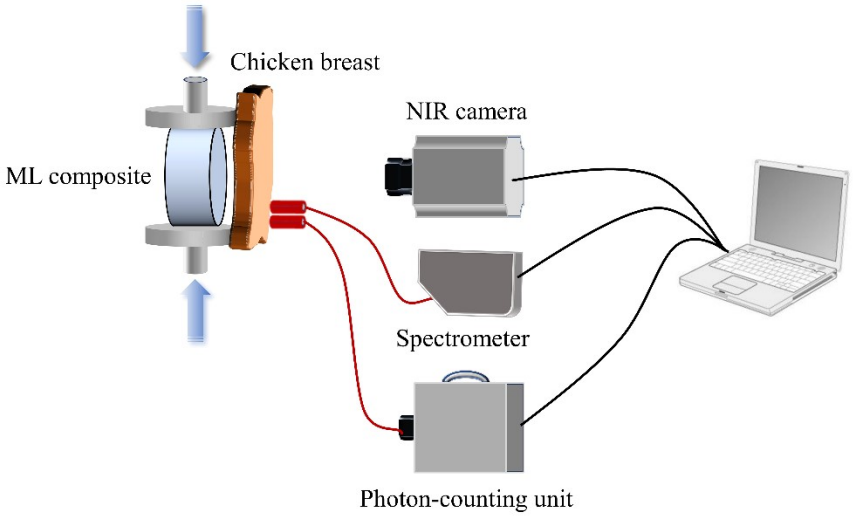

Fig. S8 Schematic illustration of the devices for mechanical application and photodetection of compression-induced NIR ML penetration across biological tissues.

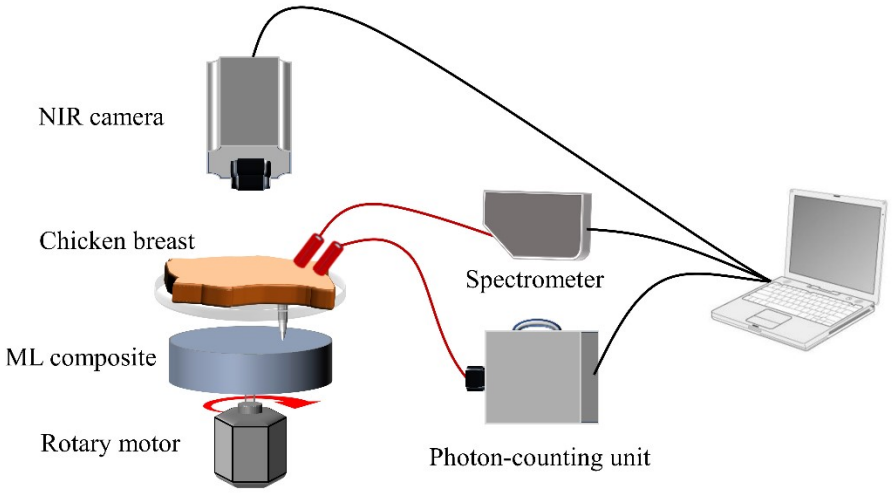

Fig. S9 Schematic illustration of the devices for mechanical application and photodetection of friction-induced NIR ML penetration across biological tissues.

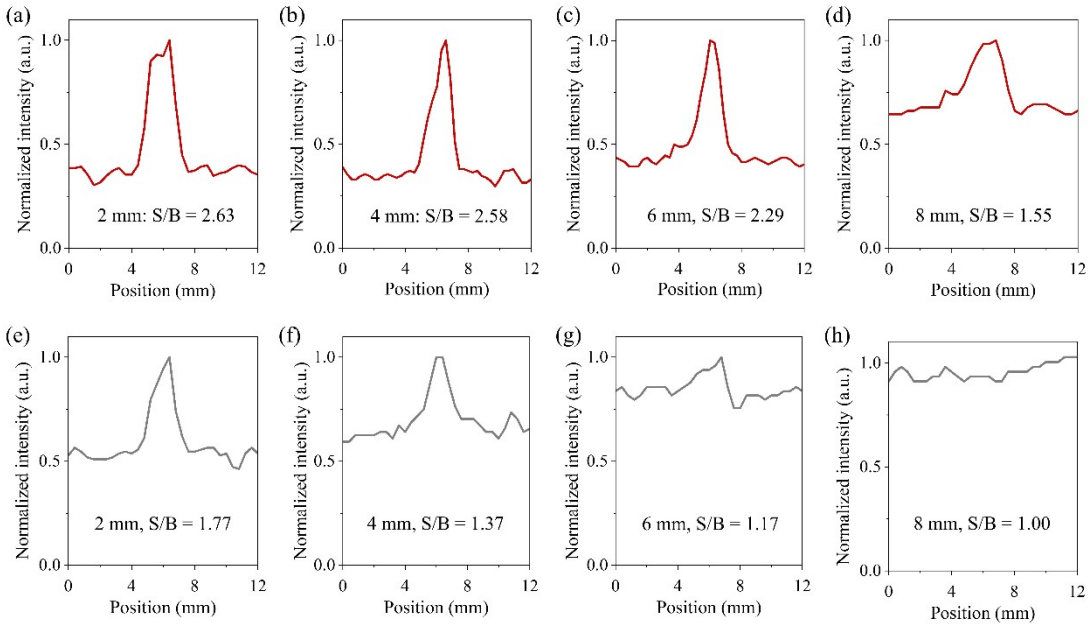

Fig. S10 SBR analysis of Fig. 5(a) in the main text. (a-d) for a CaZnOS:0.5%Nd^{3+},0.5%Mn^{2+} composite covered by chicken breasts with thicknesses of 2, 4, 6 and 8 mm, respectively. (e-h) for a CaZnOS:0.5%Nd^{3+} composite covered by chicken breasts with thicknesses of 2, 4, 6 and 8 mm, respectively. The results show that the SBR values of NIR ML images obtained using CaZnOS:0.5%Nd^{3+},0.5%Mn^{2+} are consistently higher than those using CaZnOS:0.5%Nd^{3+} when covering the same thickness of chicken tissues.

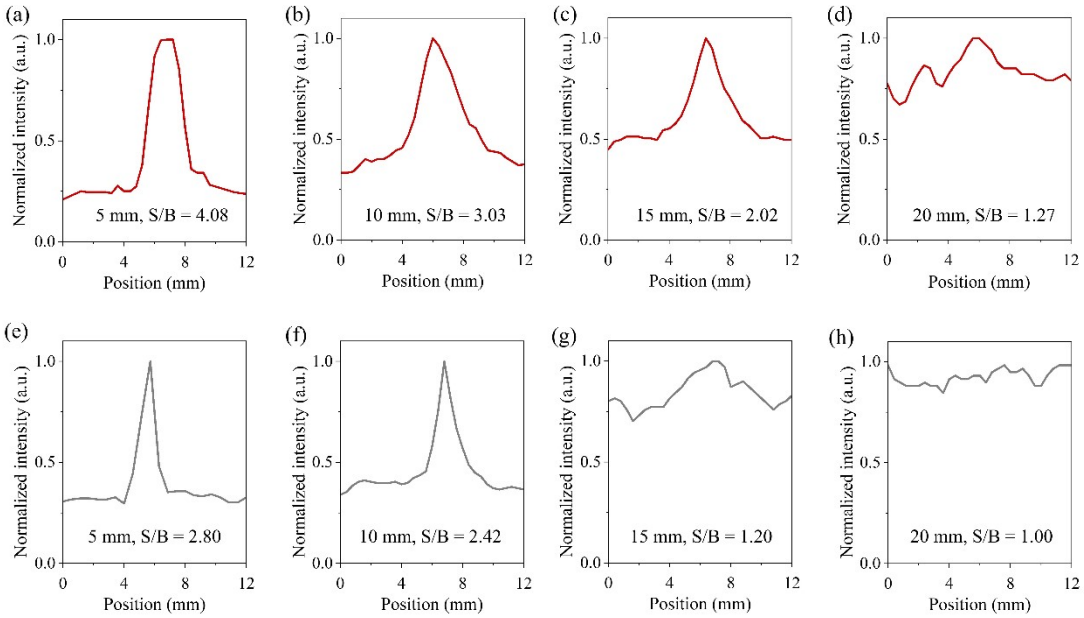

Fig. S11 SBR analysis of Fig. 5(d) in the main text. (a-d) for a CaZnOS:0.5%Nd^{3+},0.5%Mn^{2+} composite covered by chicken breasts with thicknesses of 5, 10, 15 and 20 mm, respectively. (e-h) for a CaZnOS:0.5%Nd^{3+} composite covered by chicken breast with thicknesses of 5, 10, 15 and 20 mm, respectively. The results show that the SBR values of NIR ML images obtained using CaZnOS:0.5%Nd^{3+},0.5%Mn^{2+} are consistently higher than those using CaZnOS:0.5%Nd^{3+} when covering the same thickness of chicken tissues.

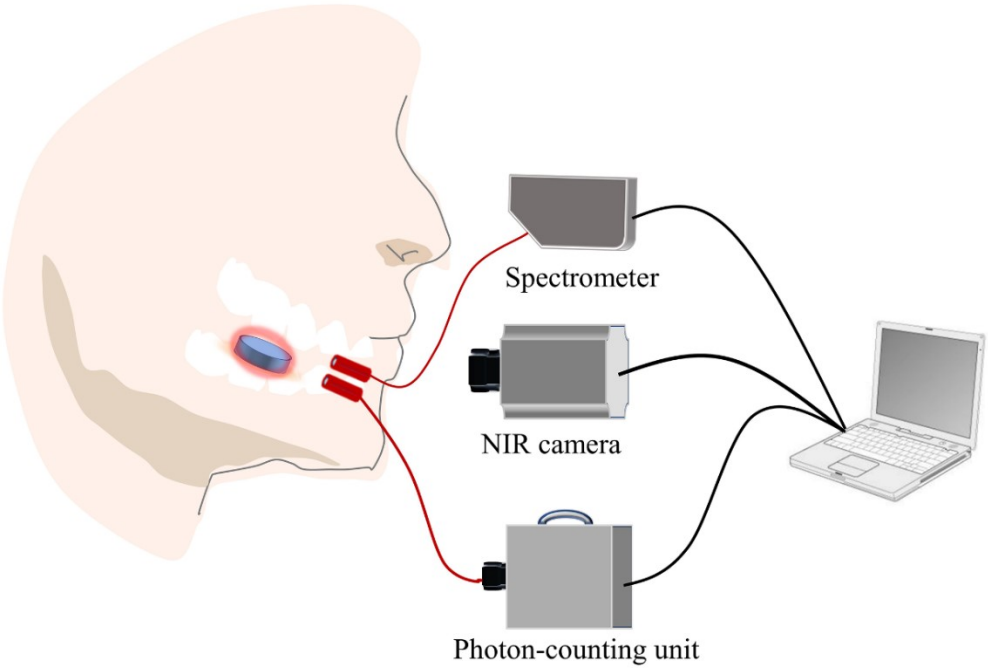

Fig. S12 Schematic illustration of the bite scene and photodetection setup for bite-induced NIR ML penetration across human cheek. Notably, the probes of the spectrometer and photon-counting unit are placed on the outside of the cheek.

Table S1. Fluorescent decay parameters of CaZnOS:Nd^{3+},Mn^{2+} series.

Component	Wavelength (nm)	A_1	τ_1 (ms)	A_2	τ_2 (ms)	R^2	τ^* (ms)
0.5%Nd	914	4628.1	0.213	268.1	1.978	0.9967	0.829
0.5%Nd,0.1% Mn	914	3502.0	0.293	681.1	1.877	0.9951	1.108
0.5%Nd,0.3%Mn	914	3252.1	0.316	547.8	2.203	0.9926	1.319
0.5%Nd,0.5%Mn	914	2483.4	0.302	647.0	1.928	0.9890	1.369
0.5%Nd,0.7%Mn	914	2944.4	0.332	667.5	2.094	0.9923	1.335
0.5%Nd,1.0%Mn	914	2744.6	0.307	572.2	2.050	0.9889	1.321
0.5%Mn	605	0.079	0.166	0.915	2.597	0.9984	2.584
0.5%Mn,0.5%Nd	605	0.256	0.561	0.673	2.236	0.9983	2.073

The experimental data was fitted according to the formula: $I(t) = A_1 exp(-t/\tau_1) + A_2 exp(-t/\tau_2)$, where $I(t)$ is the luminescent intensity, t is time, A_1 and A_2 are the different fitting values, τ_1 and τ_2 are the decay time for the exponential components. τ^* is the average decay time, which is calculated by the quadratic formula: $\tau^* = (A_1\tau_1^2 + A_2\tau_2^2)/(A_1\tau_2 + A_2\tau_2)$.